KIM, S. H. & JEFFREY, G. A. (1967). *Acta Cryst.* **22**, 537-545.
LEMIEUX, R. U. & CHU, N. J. (1958). Abstr. 133rd National Meeting of the American Chemical Society, San Francisco, p. 31.
LEMIEUX, R. U., PAVIA, A. A., MARTIN, J. C. & WANATABE, K. A. (1969). *Can. J. Chem.* **47**, 4427-4439.
LINNETT, J. W. (1960). *Wave Mechanics and Valency.* London: Methuen.
OHANESSIAN, J., LONGCHAMBON, F. & ARENE, F. (1978). *Acta Cryst.* B**34**, 3666-3671.
STEWART, R. F. & COPPENS, P. (1968). Abstr. ACA Winter Conference, Tucson. Paper G5.
TAKAGI, S. & JEFFREY, G. A. (1977). *Acta Cryst.* B**33**, 3510-3515.
TAKAGI, S., NORDENSON, S. & JEFFREY, G. A. (1979). *Acta Cryst.* B**35**, 991-993.
TVAROSKA, I. & KOZAR, T. (1980). *J. Am. Chem. Soc.* **102**, 6929-6936.
WHANGBO, M. H. & WOLFE, S. (1976). *Can. J. Chem.* **54**, 963-968.
WILLIAMS, J. O., SCARSDALE, J. N., SCHAFER, L. & GEISE, H. J. (1981). *J. Mol. Struct.* **76**, 11-28.
WOLFE, S., WHANGBO, M. H. & MITCHELL, D. J. (1979). *Carbohydr. Res.* **69**, 1-27.

Acta Cryst. (1985). B**41**, 56-66

X-ray, Neutron and Electron Diffraction Study of the One-Dimensional Organic Conductor: Trimethylammonium 7,7,8,8-Tetracyano-*p*-quinodimethane Iodine, TMA–TCNQ–I. Structure and Distortion of the Lattice, Temperature and Irradiation Effects

BY B. GALLOIS AND J. GAULTIER

Laboratoire de Cristallographie, LA 144, *associé au CNRS, Université de Bordeaux* I, 33405-*Talence CEDEX, France*

T. GRANIER AND R. AYROLES

Laboratoire d'Optique Electronique du CNRS, 29 *rue Jeanne Marvig, BP* 4347, 31055-*Toulouse CEDEX, France*

AND A. FILHOL

Institut Laue Langevin, 156 *X, Centre de Tri,* 38042-*Grenoble CEDEX, France*

(*Received* 17 *January* 1984; *accepted* 25 *September* 1984)

Abstract

According to the literature, TMA-TCNQ-I crystals show a monoclinic organic host lattice and a triclinic iodine lattice. The structure is a packing of parallel segregated regular columns of the three ions. The compound undergoes successively a 'metal-insulator' phase transition ($T_1 \sim 150$ K) associated with a Peierls-like lattice distortion and a less well understood structural transition ($T_2 \sim 95$ K). The present paper provides a new description of the 300 K structure of TMA-TCNQ-I and its structural evolution with temperature. Crystallographic data include X-ray and neutron diffraction results as well as those of the first successful electron-microdiffraction study of such an organic conductor. It is shown that the organic and the iodine lattice are both triclinic twinned and with non-parallel axes. The TCNQ columns are thus no longer regular but weakly dimerized. From examination of the neutron intensities of a number of satellite reflections, the lattice distortion below T_1 is found to be mainly transverse ($\sim 0{\cdot}06$ Å). It is helicoidal along the y axis with pitch $3b$ with right section an ellipse of major axis parallel to **a**. Three phase transitions, instead of two presently recognized, have been characterized as follows: $T_1 \sim 150$ K: satellites with the wave vector $\pm(a^*, b^*/3, c^*)$; $T_2 \sim 95$ K: the wave vector is now $\pm(\xi a^*, b^*/3, c^*)$ with ξ continuously increasing from 0 to a locking value $\xi_l = \frac{1}{6}$ at $T_3 \sim 65$ K. Lastly, the irradiation effect on the iodine lattice and the charge-density waves are described.

Introduction

Crystals of the ternary salts of the general formula $[R\text{-}(CH_3)_2N^+H]_3(TCNQ)_3^{2-}(I_3)^-$ are one-dimensional (1D) conductors; which have a 'metal-insulator' phase transition at high temperature. This behaviour is associated with the existence of parallel columns of $TCNQ^-$ molecular ions. These salts are also isostructural (Dupuis, Flandrois, Delhaes & Coulon, 1978); this characteristic has already made it possible to establish the influence of Coulombic interactions between columns on their transport properties, and in particular on the 'metal-insulator' transition temperature (Coulon, Flandrois, Delhaes, Hauw & Dupuis, 1981).

$TMA^+ (TCNQ)^{2/3-}(I_3^-)_{1/3}$, the first salt in this series to be synthesized, is also the one most studied to date. Its longitudinal electrical conductivity is relatively modest and varies significantly from sample to sample

0108-7681/85/010056-11$01.50

($\sigma_{\parallel 300\,K} = 20$ to $40\ \Omega^{-1}\ cm^{-1}$). Its behaviour as a function of temperature shows an anomaly at $T \sim 150$ K, and has either a very broad maximum at about 240 K (Abkowitz, Epstein, Griffiths, Miller & Slade, 1977), or a saturation in the vicinity of ambient temperature (Cougrand, Flandrois, Delhaes, Chasseau, Gaultier & Miane, 1976).

The structural analysis of the first samples of TMA-TCNQ-I synthesized (Cougrand *et al.*, 1976; Filhol, Rovira, Hauw, Gaultier, Chasseau & Dupuis, 1979; Filhol & Gaultier, 1980) indicated the existence of an *ordered host lattice* (*A*) of monoclinic symmetry (TMA^+ and $TCNQ^-$ molecular ion lattice) and of a *disordered lattice* (*B*) attributed to the iodine atoms. Thus the X-ray diffraction patterns showed the presence of lattice (*A*) Bragg spots and diffuse layers of high intensity parallel to the plane a^*c^* of the organic lattice and modulated in the direction $\mathbf{a}^*$. In the proposed formalism the periods of the iodine and organic lattices were $b_I^* = \frac{2}{3}b^*$ along the chain axis and the structure of the lattice (*B*) had thus been determined on the hypothesis that lattices (*A*) and (*B*) were of identical symmetry, using a model of statistical position disorder. Independently of this, the quantitative analysis of the diffuse scattering had led to a description of the iodine chains and of the interchain disorder (Filhol *et al.*, 1979).

Samples showing a quasi-ordered iodine lattice were subsequently synthesized. Coppens, Leung, Murphy, Tilborg, Epstein & Miller (1980) then showed that the lattice symmetry (*B*) of the iodines is triclinic but they did not cast doubt on the monoclinic symmetry of the organic lattice.

In fact none of the above descriptions of the structure is really satisfactory. They all show columns of TCNQ anions characterized by a regular, zigzag type stacking with excellent overlap of adjacent molecules and a small interplanar distance (3·22 Å at 300 K), although the longitudinal electrical conductivity is poor in comparison with that of other TCNQ salts having regular stacking, such as: $\sigma_{\parallel 300\,K} \sim 200\ \Omega^{-1}\ cm^{-1}$ for acridinium $(TCNQ)_2$; $100\ \Omega^{-1}\ cm^{-1}$ for quinolinium $(TCNQ)_2$; $200\ \Omega^{-1}\ cm^{-1}$ for *N*-methylphenazinium TCNQ (Shchegolev, 1972). Another surprising aspect of the proposed structure is the fact that the TCNQ molecular ions are strictly planar and parallel, as they are located on mirror planes *m* of the monoclinic lattice of symmetry $C2/m$. The TMA cations are themselves very symmetrical. In fact this is not in accordance with the observation that TCNQ anions are non-planar and more or less inclined to the stacking axis for the majority of TCNQ salts of known structure.

Here we present new X-ray and neutron diffraction data on samples with quasi-3D order, and results of electron microdiffraction giving the crystallographic information necessary for a more satisfactory description of the structure of TMA-TCNQ-I. In earlier studies this information was masked by the disorder of the iodine lattice. The new structure proposed casts doubt on the monoclinic symmetry of the organic lattice (and therefore on the high symmetry of the molecular ions) and permits a much easier interpretation of the relationship between physical and structural properties of the compound.

Experimental part

Three types of samples were studied: (i) totally hydrogenated [TMA-TCNQ-I(h_{14})]; (ii) totally deuterated: [(TMA-TCNQ-I(d_{14})]; (iii) partly deuterated: [TMA(h_{10})-TCNQ(d_4)-I]. In all cases, the single crystals were obtained by controlled cooling of a saturated solution of the compound in acetonitrile.

X-ray diffraction

X-ray diffraction patterns of the TMA-TCNQ-I samples were first recorded at room temperature by film methods in order to characterize both sublattices. All sample types (i, ii, iii) give a diffraction pattern characteristic of a quasi-3D-ordered structure, *i.e.* the iodine sublattice, Bragg reflections on which low diffuse scattering intensity is superimposed. An investigation carried out in the temperature range 100–300 K (Laue, Weissenberg and precession cameras) made it possible to follow the structural trend and in particular showed the existence of clear superstructure reflections at 100 K. This contrasts with the earlier studies which dealt with crystals showing a disordered iodine lattice.

Electron diffraction

Electron microdiffraction gives information comparable with that from X-ray diffraction. However, it permits the study of crystalline areas of very small dimensions (a few hundred Å) and the detection of structural phenomena of very low intensity. In addition the short wavelength of the electrons ($\lambda_e =$ 0·0054 Å with an accelerating voltage of 2000 kV) makes it possible to observe a large area of reciprocal space.

The study of TMA-TCNQ-I was particularly intended to show satellites linked with lattice distortion associated with the 'metal–insulator' transition ($T_{MI} \sim 150$ K) and their change as a function of temperature and irradiation dose. The experiments were carried out between 40 and 300 K on the 3 MeV electron microscope (Laboratoire d'Optique Electronique at Toulouse) equipped with a liquid-helium-cooled sample holder. The high electron accelerating voltages (1000 and 2000 kV) were used to attenuate the irradiation effects which tend to destroy the crystalline structure of the organic compounds. The intensity of the electron beam is 10^4 times weaker than that corresponding to the usual observation con-

ditions in electron microscopy, its value being close to $1{\cdot}6\times10^{-5}$ A cm^{-2} (*i.e.* 10^{-2} e Å^{-2} s^{-1}) on the specimen.

Neutron diffraction

As iodine atoms are not large neutron scatterers, only the Bragg reflections due to the organic lattice are of notable intensity, and the information obtained therefore mainly concerns organic columns.

At low temperatures, crystals of type (i) had already been examined with the aid of a Weissenberg neutron camera (Instrument D12 at the Institut Laue-Langevin at Grenoble) and of a four-circle neutron diffractometer (Instrument D8, ILL) by Filhol, Gallois, Laugier, Dupuis & Coulon (1982). Additional measurements on D8 with similar experimental conditions in the temperature range 65 to 150 K made it possible to collect the integrated intensities of 50 satellites at 100 K, to specify the change in intensity and displacement of these satellites with temperature, and also to determine the cell parameters of the various phases observed at low temperature.

Structural description of TMA–TCNQ–I at room temperature

The examination of ordered iodine lattice (3D) samples results in a new description of the structure, which as we shall see, in conjunction with the study of the interactions between conducting chains, makes it possible to explain the physical or structural behaviour as a function of temperature.

3D iodine lattice: unit cell and twin

Precession photographs with the axes a, b and c of the monoclinic cell $C2/m$ of the crystal, being in turn oriented parallel to the beam axis, showed that the iodine lattice (B) is triclinic. It is also observed that the iodine atom lattice is twinned (Fig. 1*a*). Each $(hkl)_{B'}$ reflection has a corresponding $(hkl)_{B''}$ reflection of comparable intensity, in a symmetrical position in relation to the plane a^*c^*. The Bragg reflections of these two iodine lattices are regrouped in pairs on the layers situated at $(3n\pm1)b_I^*$ (distance between two reflections of a given pair: $a_I^*/3$; distance between two neighbouring pairs: $2a_I^*/3$) but rigorously superimposed on the layers $(3n)b_I^*$. This observation, not mentioned by Coppens *et al.* (1980) but given by Coulon (1983), is common to all the samples we have examined and therefore seems to be a specific characteristic of our material. The crystalline domains are such that their respective directions $\mathbf{b}_I$ and planes b_Ic_I are common to both lattices, their directions $\mathbf{a}_I$ being symmetrical to $\mathbf{b}_I$ (Fig. 1*b*).

The cell of the iodine lattice thus described contains two independent columns of iodine atoms parallel to the axis b_I, situated respectively at $0y0$ and $\frac{1}{2}y\frac{1}{2}$. The centres of gravity of the I_3^- ions, of periodicity b_I, are $b/4$ (*i.e.* $b_I/6$) from the TCNQ planes. They are either above (columns $0y0$, $0y1$, $\frac{1}{2}y\frac{1}{2}$) or below (columns $1y0$, $1y1$) the TCNQ plane located at $y=0$. The parameters of the triclinic cell of the iodine lattice (B) are: $a_I=10{\cdot}67$, $b_I=9{\cdot}68$, $c_I=25{\cdot}24$ Å, $\alpha_I=90{\cdot}00$, $\beta_I=93{\cdot}6$, $\gamma_I=107{\cdot}6°$. In comparison with the $C2/m$ structure previously proposed, the direction $\mathbf{a}_I$ situated in the plane is inclined by 17·6° to $\mathbf{a}$, the directions $\mathbf{b}$ and $\mathbf{b}_I$ being combined, and the angle between the directions $\mathbf{c}$ and $\mathbf{c}_I$ is close to 21·4° (Fig. 2*a* and *b*). These results are in agreement with those of Coppens *et al.* (1980).

Redefinition of the organic lattice

The coexistence of a twinned iodine (B) sublattice and a non-twinned host lattice (A) appears somewhat improbable. We have therefore proposed the existence of a twin of the same type for the lattice (A), a hypothesis which is justified *a posteriori* by the fact that it is necessary to the interpretation of the results for the low-temperature phases of the compound.

The introduction of the a^*c^* twin plane for the lattice (A) leads us to consider the triclinic cell described in Table 1. The Bragg reflections of the

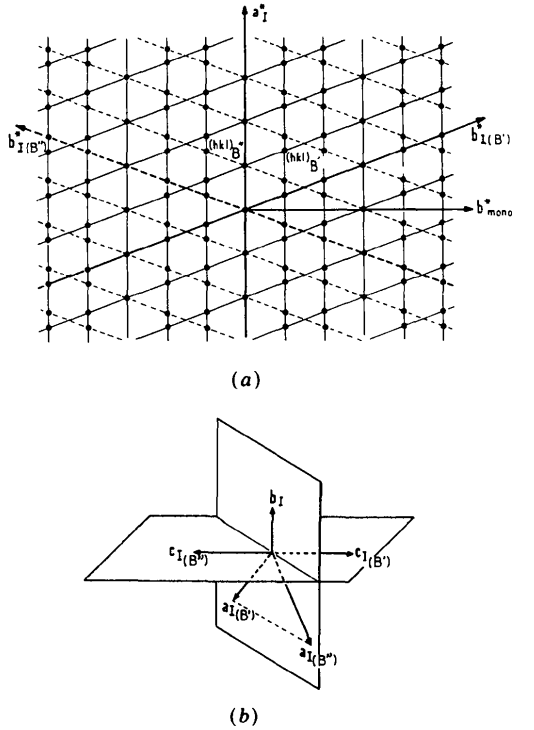

Fig. 1. (*a*) Plane $hk0$ of the ordered iodine lattice (B), showing the twin. The $\mathbf{a}_I^*$ directions for each domain are indistinguishable, the $\mathbf{b}_I^*$ directions are symmetrical with respect to $\mathbf{a}_I^*$. (*b*) Twin of the iodine lattice (B). Definition in real space of the axial system of each domain.

reciprocal lattices (A') and (A'') of the two crystalline domains are rigorously superimposed in pairs but are not equivalent. They correspond to the respective indices $(h, k, l)_{A'}$ and $(h+k, \bar{k}, l)_{A''}$ (Fig. 3). In other words the monoclinic lattice $C2/m$ used up to the present corresponds to the superimposition of two lower-symmetry lattices and the arrangement of the molecular ions TCNQ, described in the monoclinic cell, is therefore a 'mean' arrangement. The triclinic symmetry itself no longer requires the TCNQ to be planar, equidistant in the columns and perpendicular to **b** (omission of mirror m), and the stacking in the columns is therefore no longer strictly regular but is dimerized. This dimerization is not very marked, as is shown by the thermal atomic motion ellipsoids calculated in the symmetry $C2/m$ (Filhol *et al.*, 1979) which have no major anomalies.

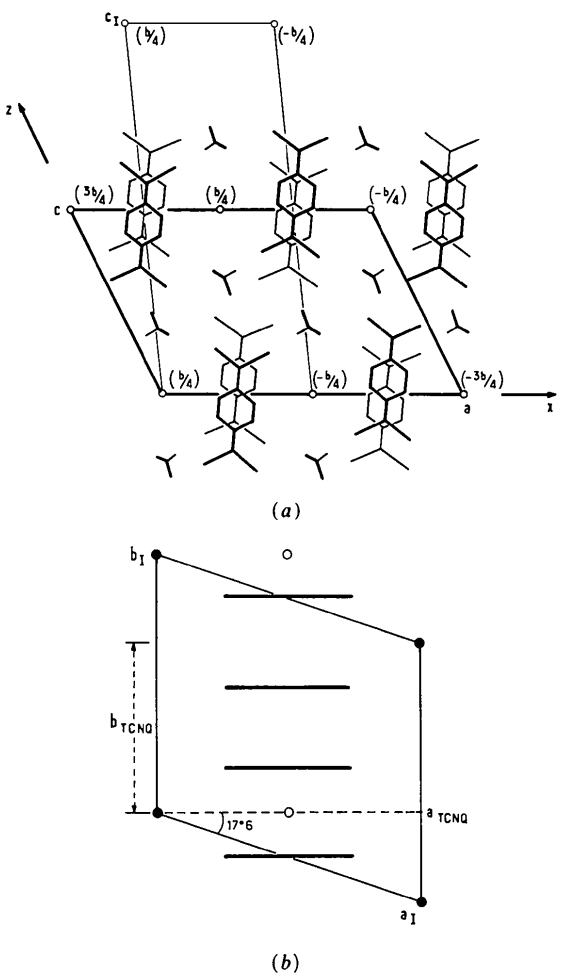

Fig. 2. (*a*) Projection along **b** of the structure of TMA-TCNQ-I. Monoclinic organic unit cell (thick line) and definition of the triclinic unit cell of the iodine lattice (thin line). ○: Centres of mass of the I_3^- ions. $\mathbf{a}_I = \frac{1}{2}(\mathbf{a}-\mathbf{b})$; $\mathbf{a}_I$ outside the monoclinic *ac* plane. $\mathbf{b}_I = \frac{3}{2}\mathbf{b}$; $\mathbf{b}_I$ parallel to **b**. $\mathbf{c}_I = \mathbf{a}/2+2\mathbf{c}$; $\mathbf{c}_I$ in the *ac* plane. (*b*) Positions of the I_3^- ions with respect to the TCNQ planes (thick line) perpendicular to the **b** direction: $\mathbf{b}_I$ and **b** are collinear, $\mathbf{a}_I$ is inclined at 17·6° to **a**. ●: centres of mass of the I_3^- ions of the column $0y0$, $1y0$ and $0y1$. ○: centres of mass of the I_3^- ions of the columns $\frac{1}{2}$, y, $\frac{1}{2}$.

Table 1. *Unit-cell parameters of* TMA-TCNQ-I *in the old (monoclinic) and new (triclinic) symmetry*

	Monoclinic $C2/m$ symmetry*	Triclinic symmetry		
	300 K	300 K	100 K	65 K
a (Å)	20·353	10·676	10·632	10·570
b (Å)	6·456	6·456	6·364	6·355
c (Å)	13·922	13·922	13·703	13·660
α (°)	90·0	90·0	90·0	90·7
β (°)	115·2	113·9	113·2	112·9
γ (°)	90·0	107·6	108·2	107·4
V (Å^3)	1655·0	827·7	801·7	796·7

* Filhol *et al.* (1979).

In this new structural model, the axes of the cell of the organic lattice (A) and of the cell of the iodine lattice (B) are not parallel. Using subscripts t and I for triclinic lattices (A) and (B) respectively of a given crystal domain, $\mathbf{a}_t$ is parallel to $\mathbf{a}_I$, and $\mathbf{b}_t$ is parallel to $\mathbf{b}_I$ and the corresponding periods are commensurable: $\mathbf{a}_t = \mathbf{a}_I$; $\mathbf{b}_t = \frac{2}{3}\mathbf{b}_I$. The directions $\mathbf{c}_t$ and $\mathbf{c}_I$ are separated by 21·40°; $\mathbf{c}_t = \frac{1}{2}(\mathbf{c}_I - \mathbf{a}_I - \frac{1}{3}\mathbf{b}_I)$. This new approach to the structure of the organic lattice of TMA-TCNQ-I is more satisfactory as regards the structural observations effected on other TCNQ salts and takes better account of the relatively low longitudinal electric conductivity of the compound. In fact the analogy can be made in particular with the salts of the radical cation TMTTF (Flandrois, Coulon, Delhaes, Chasseau, Hauw, Gaultier, Fabre & Giral, 1981), which exhibit both a dimerized stacking and a 1D metallic behaviour which is the more marked the stronger the interchain interactions. This agrees with the observation for TMA-TCNQ-I of very marked 1D electronic character and slightly metallic behaviour (Filhol *et al.*, 1982).

New approach to the quasi-1D ordered iodine lattice

The analysis by X-ray scattering of the disorder affecting the iodine chains has already been published

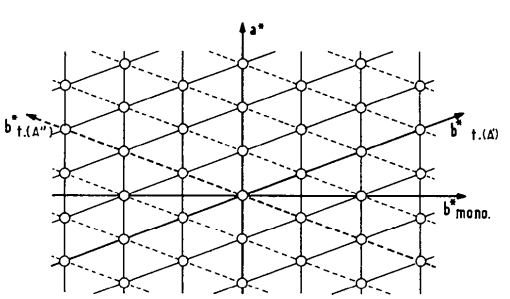

Fig. 3. Organic reciprocal lattice (A). The Bragg reflections of the twins (A') and (A'') are superimposed in pairs, but the corresponding Miller indices are different.

by Filhol *et al.* (1979). This was based on the evaluation of the relative intensities of the diffuse layer lines measured on a rotating *b*-axis crystal pattern. In the model proposed by the authors, the longitudinal displacement was assumed to be random (no interchain correlations) and was described by two parameters d and ε indicating respectively the presence of I_3^- ions and of the shift of the chains relative to the mean position. The results obtained appear satisfactory (I_3^- ions of length $d = 6{\cdot}00$ Å; distance between ions: 3·68 Å and displacement $\varepsilon \sim 0{\cdot}08$ Å) but do not explain either the existence of two families of diffuse layers of different types or the modulation of their intensity in the **a*** direction.

A first family L_1 of layers, situated at $(3n \pm 1)2b^*/3$, presents maxima of intensity spaced at $2a^*$. The layer lines L_2 situated at $(3n)2b^*/3$ show maxima also spaced by $2a^*$, but shifted by a^* from the previous ones and superimposed on continuous diffuse scattering. These layers (Fig. 4) show a considerable difference in the distribution of the diffuse scattering. These observations are now explained by the co-existence of crystalline domains (B') and (B'') of the twin.

In the case of disordered crystals, the Bragg spots on a reciprocal plane are replaced by diffuse spots. On the layers L_1, these spots are partially superimposed to give longer diffuse regions with a maximum of intensity at $(n+\frac{1}{6})a_I^*$, the periodicity a_I^* of which leads to an identical modulation of diffuse intensity for each layer line. For the layers of type L_2, the diffuse spots of each sublattice are superimposed resulting in more localized diffuse intensity of which the maximum is at na_I^* and has the same periodicty as layers L_1.

These diffuse layer lines L_1 and L_2 have an intensity modulated only along **a***, indicating the existence of short-range correlations (several iodine chains) in the direction **a** and the absence of correlations along **c**. On the other hand the diffuse layer lines are not broader than the Bragg peaks and the axial coherence length of the iodine chains is thus very high. This last observation is in contrast with an erroneous value (150 ± 30 Å) previously proposed by Filhol *et al.* (1979).

Structural changes in the organic lattice with temperature

The variation with temperature of the physical properties of ordered iodine lattice TMA-TCNQ-I shows two anomalies (Fig. 5). The first ($T_1 \sim 150$ K), found particularly in the course of the study of electrical conductivity, was attributed to a 'metal-insulator' phase transition by Coulon *et al.* (1981). The second ($T_2 \sim 90$ K), corresponding to a marked minimum of Young's modulus at this temperature, was attributed by Brill, Epstein & Miller (1979) to the freezing out of the methyl groups of the TMA cation.

Temperature dependence of the wave vector **q** *of the lattice distortion*

The structural transitions at T_1 and T_2 were first analysed by Filhol *et al.* (1982), and in more detail by Gallois, Gaultier, Pouget, Coulon & Filhol (1983) and Gallois, Coulon, Pouget, Filhol & Dupuis (1984).

For $T < T_1$, the neutron diffraction data (Filhol *et al.*, 1982) show for the 3D-order compound the existence of superstructure reflections of low intensity. The components of wave vector **q** associated with the distortion of the lattice, expressed in monoclinic and triclinic cells, are (a^*, $\pm b^*/3$, c^*) and ($\pm a_t^*/6$, $\pm b_t^*/3$, c_t^*) respectively. The superstructure intensities are at a maximum at about 100 K.

Electron microdiffraction observations have confirmed the above results: the satellites are clearly visible on the photographs obtained for $T < 150$ K

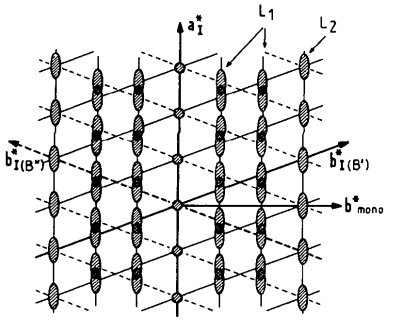

Fig. 4. *hk*0 plane of the disordered iodine lattice. The analogy with the plane *hk*0 of the ordered lattice (Fig. 1*a*) facilitates the comprehension of the diffuse scattering characterizing the layer groups L_1 and L_2. Layers L_1: the maxima are at $(n+\frac{1}{6})a_I^*$. Layers L_2: the maxima are at na_I^*.

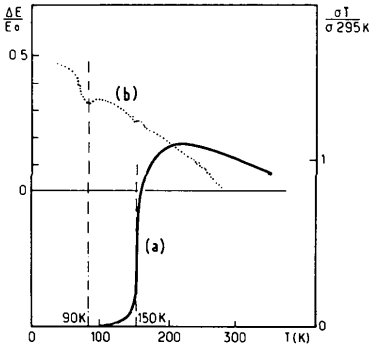

Fig. 5. Physical properties of TMA-TCNQ-I as a function of temperature. (*a*) Electrical conductivity parallel to the chain axis of the ordered compound, and anomaly at $T \sim 150$ K (according to Abkowitz *et al.*, 1977). (*b*) Changes in the Young modulus and anomaly at $T_2 \sim 90$ K (according to Brill *et al.*, 1979).

(Fig. 6*a* and *b*). This technique has provided access to two new items of information:

(*a*) At 100 K there are additional low-intensity reflections at 0, $\pm 2b^*/3$, 0 (Fig. 6); these are visible for numerous sample orientations, except for the plane a^*b^*. They could correspond to satellite or harmonics of the TCNQ lattice rather than of the iodine lattice since their $\mathbf{a}^*$ component is zero.

(*b*) The appearance below 95 K of a non-zero ξ component along $\mathbf{a}^*$ of the wave vector. The analysis of the patterns obtained between 40 and 100 K shows that ξ changes continuously (Fig. 7) from $\xi = 0$ to a limiting value $\xi_l \sim (\frac{1}{6} \pm 0{\cdot}016)$ reached at ~70 K. Filhol *et al.* (1982) pointed out a considerable decrease in satellite intensity below 100 K. We thus confirm that, among the hypotheses advanced by these authors to explain this surprising result, the truncating effect associated with the displacement of the wave vector of satellites is the correct one.

Table 2. *Satellite wave-vector changes as a function of temperature*

	Triclinic symmetry	Monoclinic $C2/m$ symmetry
150 K > T > 95 K	$(-\frac{1}{6}\mathbf{a}_t^*, \pm\mathbf{b}_t^*/3, \mathbf{c}_t^*)$	$\pm(\mathbf{a}^*, \mathbf{b}^*/3, \mathbf{c}^*)$
95 K > T > 65 K	$(\xi'\mathbf{a}_t^*, \pm\mathbf{b}_t^*/3, \mathbf{c}_t^*)$	$(\xi\mathbf{a}^*, \pm\mathbf{b}^*/3, \mathbf{c}^*)$
	$\frac{1}{12} < \xi' < \frac{1}{6}$	$0 < \xi < \frac{1}{6}$
$T \leq 65$ K	$(\mathbf{a}_t^*/12, \pm\mathbf{b}_t^*/3, \mathbf{c}_t^*)$	$(\mathbf{a}^*/6, \pm\mathbf{b}^*/3, \mathbf{c}^*)$

Neutron-diffraction measurements subsequently confirmed that the wave-vector component ξ along $\mathbf{a}^*$ assumes a non-zero value from $T_2 = 95 \pm 1$ K to $T_3 = 65 \pm 1$ K where it locks on the value $\xi_l = (0{\cdot}161 \pm 0{\cdot}006)$ (Fig. 7). These last measurements have also confirmed, in agreement with the results obtained by electron microdiffraction, that the satellite displacement is limited to the a^*b^* plane, since no $\mathbf{c}^*$ component has been discovered. The changes in the wave vector as a function of temperature, expressed in both the monoclinic and triclinic reference axes, are summarized in Table 2.

For $T > 150$ K, whatever the diffraction technique used, we were not able to show pre-transitional effects. However, in neutron diffraction the changes in intensity of the superstructure reflections as a function of the temperature (Filhol *et al.*, 1982) show that the intensity is not zero between 150 and 170 K. This observation suggests the existence of precursors, the

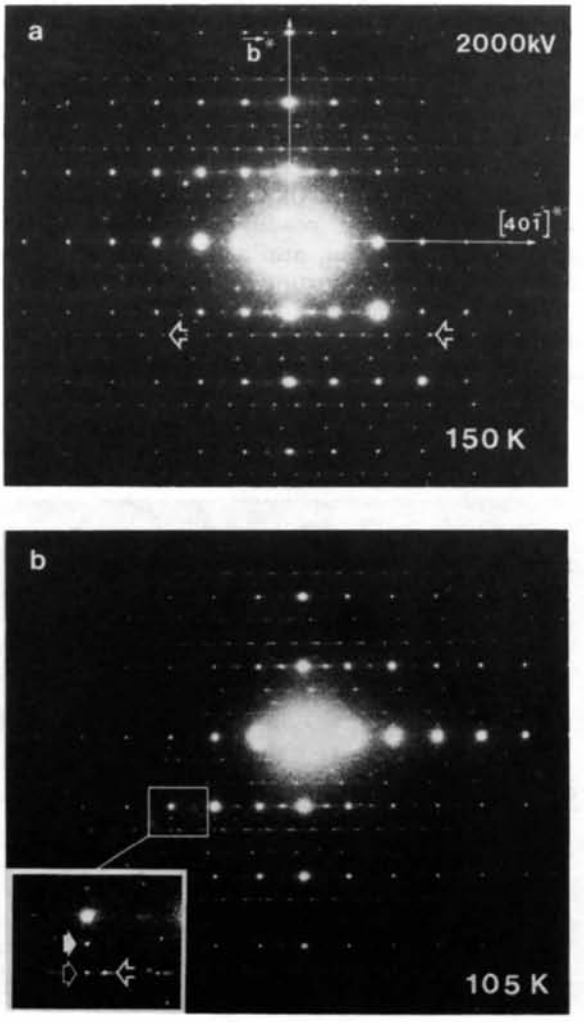

Fig. 6. Electron microdiffraction diagram of TMA-TCNQ-I taken at 2000 kV. (*a*) $T \sim 150$ K: plane $\{[40\bar{1}]\,.\,\mathbf{b}^*\}$. The diffraction peaks of the iodine lattice (hollow arrows) are at $\frac{2}{3}b^*$ from the organic lattice ones. (*b*) $T \sim 105$ K: plane $\{[40\bar{1}]\,.\,\mathbf{b}^*\}$. The satellites (solid arrows) are visible at $\pm\frac{1}{3}b^*$ and are accompanied by a second series of reflections at $\pm\frac{2}{3}b^*$ (fine hollow arrows) with the same component in the direction $[40\bar{1}]$.

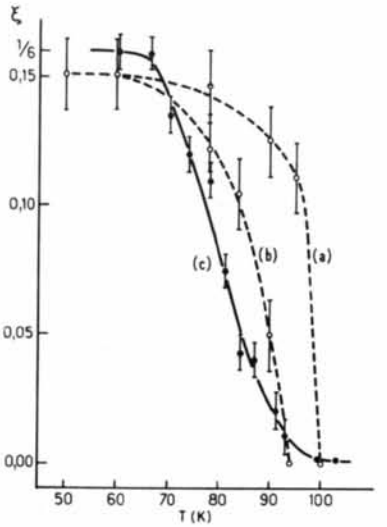

Fig. 7. Changes in the $\mathbf{a}^*$ component (ξ) of the distortion wave vector as a function of temperature. Curves (*a*) and (*b*) obtained by electron microdiffraction correspond to measurements made on two different crystals. Curve (*c*) shows neutron diffraction results. (The difference found in temperature between electron microdiffraction and neutron diffraction may be explained by poor thermal contact between sample and sample holder, in the case of the former technique.)

1D or 3D character of which has not been clarified by this method while pre-transitional effects have finally been observed by X-ray scattering (Coulon, 1983; Gallois *et al.*, 1983). Surprisingly for this type of transition, they are three-dimensional, present over a very small temperature range and not very intense, this being interpreted as a consequence of a linear coupling between fluctuations of the order parameter of the organic chain distortion and iodine lattice fluctuations (soft mode at $b^*/3$). The lattice distortion at $T_1 \sim 150$ K is then, according to the authors, a '*generalized*' *Peierls* transition.

Cell evolution

The cell parameters, corresponding to the reflections of the organic lattice (A), evolve continuously down to $T_2 \sim 95$ K with, however, a change of slope at $T_1 = 150$ K reported by Coulon *et al.* (1981). The cell parameters at 100 and 300 K, referred to the triclinic cell, are indicated in Table 1. In this temperature range, only β_t and γ_t vary significantly (0·8 and 0·6° respectively), implying a relative longitudinal shift of the adjacent columns in the **a** direction.

At $T_2 \sim 95$ K, neutron diffraction shows a splitting of the Bragg reflections of the principal lattice (A) and of the superstructure reflections.† This splitting occurs not only in the **c*** direction as indicated by Filhol *et al.* (1982) but also in the **a*** direction. This corresponds to a change in the cell of lattice (A): the $(hkl)_{A'}$ and $(h+k, \bar{k}, l)_{A''}$ reflections of the two twin domains are no longer strictly superimposed. The parameters of the triclinic twin (in Table 1) show that the splitting of the reciprocal-lattice points corresponds for $T \sim 65$ K to angular variations $\Delta\alpha^*$ and $\Delta\gamma^*$ of 0·65 and 0·5° respectively. The b^* axis is inclined by 0·64° in relation to its position when $T > T_2$; the angle between the directions **b*** for each domain is then 1·30°.

These observations are confirmed by the results of electron microdiffraction. The diffraction pattern in Fig. 8 shows clearly each area defined by its own 'Laue zone' [high-intensity reflections corresponding to the intersection of planes $(a^*b^*)_{t1}$ and $(a^*b^*)_{t2}$ with the Ewald sphere], and the superstructure associated with each of them. $\mathbf{a}^*_{t1}$ and $\mathbf{a}^*_{t2}$ are in opposite directions so that the component ξ along **a*** of the wave vector is inverted. The angle formed by the two planes can be deduced from the relation:

$$\Delta\theta = (D_{w_1 w_2}/D_B)\theta_B$$

where $D_{w_1 w_2}$ represents the distance between the curves of each zone axis and where D_B is the distance between the central spot and the *hkl* spot of the Bragg angle θ_B. The value obtained ($\Delta\theta \sim 1{\cdot}27°$) (Granier, 1982; Granier & Ayroles, 1983) is in good agreement with that from neutron diffraction ($\Delta\theta \sim 1{\cdot}30°$).

In direct space the variation of cell parameters involves essentially the parameters a and α, and to a lesser extent β and γ, and is interpreted by a relative slip of TCNQ columns, parallel to **b**. For the homologous columns in the **a** direction it is approximately 0·05 Å; for the homologous columns in the **c** direction it is close to 0·15 Å.

The transition at $T_2 \sim 95$ K affects essentially the elastic properties of the compound. It is probably of the order–disorder type associated with the thermally activated motion of the TMA cation. There is an associated modification of the organic lattice (A), which can only be readily interpreted in the hypothesis of the twin, and a displacement of the wave vector of the distortion. In addition, Gallois *et al.* (1983) have shown that this second transition also introduces a doubling of the periodicity of the iodine lattice (B). Finally the transition at $T_3 \sim 65$ K corresponds to the *locking* of the distortion wave vector at the value $\xi_l = \frac{1}{6}a^*$. Below this temperature, the

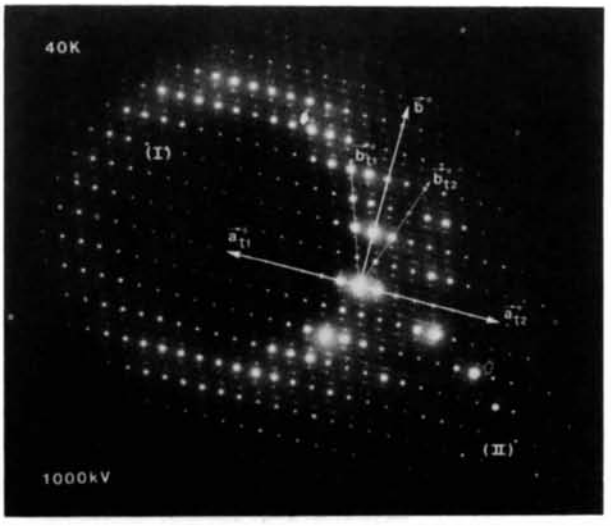

Fig. 8. Electron-diffraction diagram taken at a voltage of 1000 kV; $T \sim 40$ K. Each area (I) and (II) is characterized by the corresponding plane $a^*_I b^*_I$ and $a^*_{II} b^*_{II}$. Solid arrows: the superstructure spots relative to twin (I); hollow arrows: superstructure spots corresponding to twin (II). Their **a*** components of the superstructure spots of domains (I) and (II) are opposed and symmetrical with respect to the direction **b*** of the monoclinic lattice.

† In addition to the well known anomaly at $T \sim 150$ K in the electrical properties of TMA-TCNQ-I, Ikari, Jandl & Aubin (1983) have observed a second anomaly at 82 K (decreasing T) and 85 K (increasing T). This is ~10 K less than our value for T_2 and such a discrepancy seems beyond the estimated experimental error bars (crystal temperature ±0·5 K, transition temperature ±3 K). This suggests that structural and electrical anomalies have different origins or that sample effects (iodine disorder, purity, *etc.*..) on T_2 are large. The coincidence or non-coincidence of the starting temperatures of the reflection splitting and the a^* shift of the superlattice wave-vector parameter ξ may also be discussed. From our data both temperatures are indistinguishable within error bars.

distortion wave vector and the new direction $\mathbf{b}_I^*$ of the iodine lattice (B) are collinear. The $T_2 \sim 95$ K and $T_3 \sim 65$ K transitions certainly originate in the strengthening of the couplings between chains of molecular ions and chains of iodine atoms, when the temperature falls.

Description of distortion at $T = 100$ K

The lattice distortion below T_1 may be described for each TCNQ column as the resultant of three orthogonal $\mathbf{A}_i$ waves, one polarized longitudinally ($\mathbf{A}_2 \| \mathbf{a}$), the two others transversely. The respective amplitudes and directions can be deduced from the intensities of the superstructure reflections (Guinier, 1964).†

A *preliminary analysis* has been carried out under the hypothesis of a sinusoidal distortion affecting the TCNQ columns. If I_{TCNQ} is the contribution of the TCNQ structure factors to the intensity of a main reflection, and if s is the scattering vector of components s_a, s_b and s_c of the satellite point associated with this reflection, the superstructure intensity I_{sat} is then given by the relation:

$$\sum_i (\mathbf{A}_i \cdot \mathbf{s})^2 = \frac{1}{\pi^2} \times \frac{I_{sat}}{I_{TCNQ}}. \qquad (1)$$

The vectors $\mathbf{A}_i$ and s are expresssed in the orthogonal reference axes $\mathbf{a}^*$, $\mathbf{b}^*$, $\mathbf{a}^* \wedge \mathbf{b}^* = \mathbf{c}$ of the initial monoclinic lattices; the angle χ betweeen $\mathbf{a}^*$ and $\mathbf{A}_1$ determines the position of the orthogonal triplet ($\mathbf{A}_1$, $\mathbf{A}_2$, $\mathbf{A}_3$) in which (Fig. 9*a*):

$$\mathbf{A}_1 \cdot \mathbf{s} = A_1 s_a \cos\chi + A_1 s_c \sin\chi$$

$$\mathbf{A}_2 \cdot \mathbf{s} = A_2 s_b$$

$$\mathbf{A}_3 \cdot \mathbf{s} = -A_3 s_a \sin\chi + A_3 s_c \cos\chi.$$

The preceding relation (1) is then written:

$$A_1^2 s_a^2 + A_2^2 s_b^2 + A_3^2 s_c^2 + \{[\sin^2\chi(s_a^2 - s_c^2) - \sin 2\chi(s_a s_c)] \times (\mathbf{a}_3^2 - \mathbf{a}_1^2)\} = \frac{1}{\pi^2} \times \frac{I_{sat}}{I_{TCNQ}} \qquad (2)$$

The intensities of some superstructure reflections, and the corresponding main reflections, were measured by Filhol *et al.* (1982), by neutron diffraction. From these data we have calculated the relative contribution of the TCNQ to the total intensity on the basis of structural data at 100 K, adopting a mean Debye factor of 1·62 Å^2 for iodine, and 1·3, 0·95 and 2·2 Å^2 for the atoms of nitrogen, carbon and hydrogen

†Here a rigid displacement of molecules with no phase relations between the three orthogonal waves is assumed. Another approach is possible (Yamaji, Megtert & Comès, 1981; Yamaji, Pouget, Comès & Bechgaard, 1983) which considers only one wave with three components thus leading to satellite intensities containing interferences between the various components.

Table 3. *Data for first approach to distortion of lattice at* 100 K *- list of reflections measured*

Main reflections	Adjacent satellites	F_{TCNQ}/F_{TOTAL}	I_{sat}/I_{TCNQ}
10 0 2	10 1/3 2	0·669	0·016
9 1 6	9 4/3 6	0·620	0·034
11 1 5	11 4/3 5	1·053	0·018
6 2 4	6 7/3 4	0·748	0·020
5 3 1	5 8/3 1	0·897	0·031
11 3 5	11 8/3 5	0·850	0·017

appearing in the TCNQ groups and 1·5, 2·16 and 4·8 Å^2 for those in the TMA groups. Table 3 gives the list of reflections taken into consideration in the calculation, the contribution of the TCNQ to the structure factors and the ratio I_{sat}/I_{TCNQ}.

The most probable solution of equation (2) is obtained for (Fig. 9*b*): $|\mathbf{A}_1| \sim 0$, $|\mathbf{A}_2| \sim 0$, $|\mathbf{A}_3| \sim 0{\cdot}06$ Å; $\chi = -57{\cdot}3°$.

The distortion observed in numerous 1D conductors such as HMTTF-TCNQ (Megtert, Pouget, Comès, Garito, Bechgaard, Fabre & Giral, 1978) or TTF-TCNQ and TSeF-TCNQ (Khanna, Pouget, Comès, Garito & Heeger, 1977) have a large longitudinal component. More recently the analysis of diffuse scattering performed in TSeF-TCNQ (Yamaji *et al.*, 1981) and in HMTSeF-TCNQ (Yamaji *et al.*, 1983) showed that the major displacement is in fact *along the long directions* of the tilted molecules where it combines coherently longitudinal and transverse components. In contrast in TMA-TCNQ-I to a first

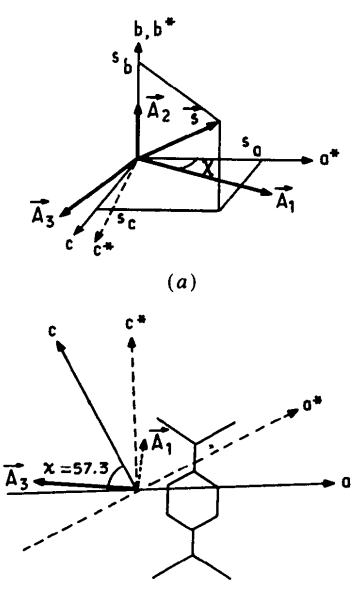

Fig. 9. (*a*) Distortion of the organic lattice (A) for $T < T_1$: definition of the reference axes of the components of the deformation wave $\mathbf{A}_1$ and $\mathbf{A}_3$ (transverse), $\mathbf{A}_2$ (longitudinal) and orientation in relation to the axes of the direct (a, b, c) and reciprocal (a^*, b^*, c^*) monoclinic unit cell. (*b*) Distortion of the organic lattice: orientation of the transverse wave $\mathbf{A}_3$ which is preponderant in the distortion of the columns of TCNQ anions.

approximation there is no longitudinally polarized wave ($|\mathbf{A}_2| \sim 0$) leading to a modulation of the interplanar spacing. The distortion is thus essentially described by the single wave $\mathbf{A}_3$ *perpendicular to the long molecular axis* (δ) of the TCNQ. The displacement of each TCNQ in the direction $\mathbf{A}_3$ determined by the angle χ is given by the equation:

$$d = A_3 \sin(2\pi qy),$$

where y represents the position of the TCNQ ion under consideration in a cell of periodicity $3b$.

A *more precise description* of the distortion was sought on the above hypothesis, from a new set of data on neutron intensities measured at 100 K (32 main reflections and 42 adjacent satellites). However, with this model it is not possible to account entirely satisfactorily for the intensities of satellites, and we have therefore used a method of rigid-body least-squares refinement* to estimate the individual displacement of the TCNQ groups. The previous model was used as a basis to limit the number of parameters to be refined.

The cell studied is triclinic $P\bar{1}$ of periods a, $3b$, c and thus contains six TCNQ moieties per column. The distortion is assumed to affect only the TCNQ stacks. As no satellite has been observed for the reflections $0k0$, despite considerable counting times, their intensity (I_{sat}) may be considered to a first approximation as zero; the relation (2) then gives $|\mathbf{A}_2|^2 = 0$. However, as the satellites at $\pm\mathbf{q}$ of the reflections $0k0$ can be observed by electron microdiffraction, a very small longitudinal component $\mathbf{A}_2$ exists; it is clearly negligible in comparison with the transverse components. The refinement is thus on the most probable displacements only, *i.e.* the translations in the *ac* plane of TCNQ molecular ions.

* *ORION* program (André, Fourme & Renaud, 1971).

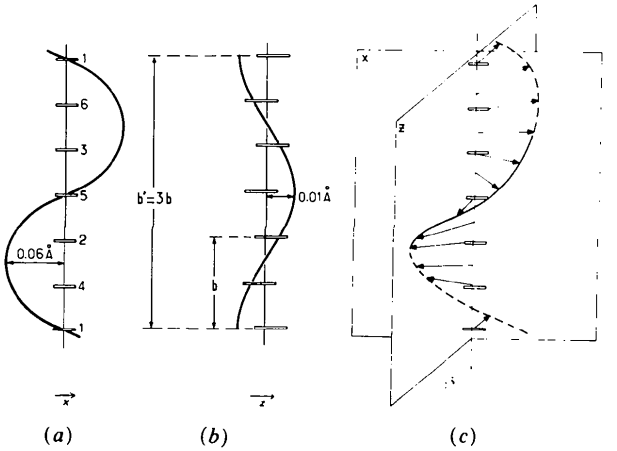

Fig. 10. Schematic illustration for a period $b' = 3b$ of the translation components of the TCNQ species within one column. (*a*) In the **a** direction of the monoclinic lattice. (*b*) In the **c** direction of the same lattice. (*c*) Resulting helicoidal distortion.

Table 4. *Observed values of displacements* (Δx *and* Δz) *of TCNQ* (*labelled in Fig.* 10) *barycentres, in relation to the axis of the chains*

Δx and Δz (in fractions of unit cell) characterize the translations in the **a** and **c** directions of the $P\bar{1}$ unit cell under consideration.

TCNQ moieties	$\Delta x(\times 10^3)$	$\Delta z(\times 10^3)$
1	−0·2	−1·0
2	−2·5	+0·6
3	+2·5	+0·6
4	−2·5	−0·6
5	+0·1	+1·0
6	+2·5	−0·6

The results obtained are shown in Table 4 and correspond to a final reliability factor $R = [\sum||F_o| - |F_c||/\sum|F_o|]$ of ~0·04. Fig. 10 shows transverse displacements of TCNQ in the directions **a** and **c**, which may be described to a first approximation as being of sinusoidal type. The equations of these displacements are thus of the form:

$$\Delta x = A \sin 2\pi qy \quad \text{with } A = 0{\cdot}06 \text{ Å}$$

$$\Delta z = B \cos 2\pi qy \quad \text{with } B = 0{\cdot}01 \text{ Å}$$

and the distortion is *helicoidal* along the y axis with pitch $3b$, and its right section is an *ellipse* with a major axis parallel to **a**. In other words, the resulting displacements (Fig. 11) are opposed in pairs (groups 1 & 5, 2 & 6, 3 & 4), nearly perpendicular to the long molecular axis for TCNQ molecules 2 & 6 and 3 & 4, and of lower amplitude and parallel to the direction **c** for the TCNQ 1 & 5.

The description of the distortion proposed here is, however, not complete. Electron microdiffraction (Granier & Ayroles, 1982, 1983) has in fact shown the presence at $\pm 2b^*/3$ of satellite harmonics. These harmonics were not observed in neutron diffraction and were therefore not taken into account in the calculation. The collection of a larger number of superstructure intensities would make it possible to eliminate the original hypotheses limiting the number of parameters to be refined and thus to include in the calculation the possible rotation of TCNQ groups and displacements of TMA groups.

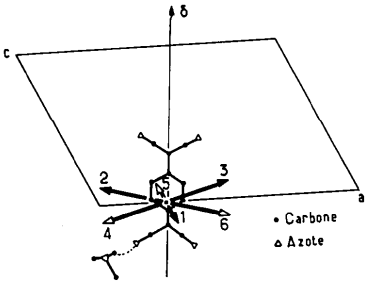

Fig. 11. Resultant direction for each TCNQ labelled in Fig. 10, of displacements in the monoclinic *ac* plane.

Effects of electron irradiation: loss of three-dimensional order

The organic crystals are very sensitive to electron irradiation, so that their observation by electron microdiffraction requires special precautions. In addition the observation of the superstructure associated with the Peierls distortion is still more sensitive to the concentration of defects in the crystal (Zuppiroli & Bouffard, 1980; Zuppiroli, Mutka & Bouffard, 1982). It was therefore necessary to study the values of the accelerating voltages (Thomas, Humphreys, Duff & Grubb, 1970; Dupouy, 1974) and of the temperature (Salih & Cosslett, 1975–1976), which were most favourable to the observation. Only at high voltage was it possible conveniently to observe superstructure spots as in this case the radiation dose received by the crystal during a photographic exposure time (30 s) may be reduced below the critical doses as discussed in the following.

The photographs in Fig. 12, taken at a voltage of 1000 kV, show for $T \sim 40$ K the changes in superstructure reflections as a function of the irradiation

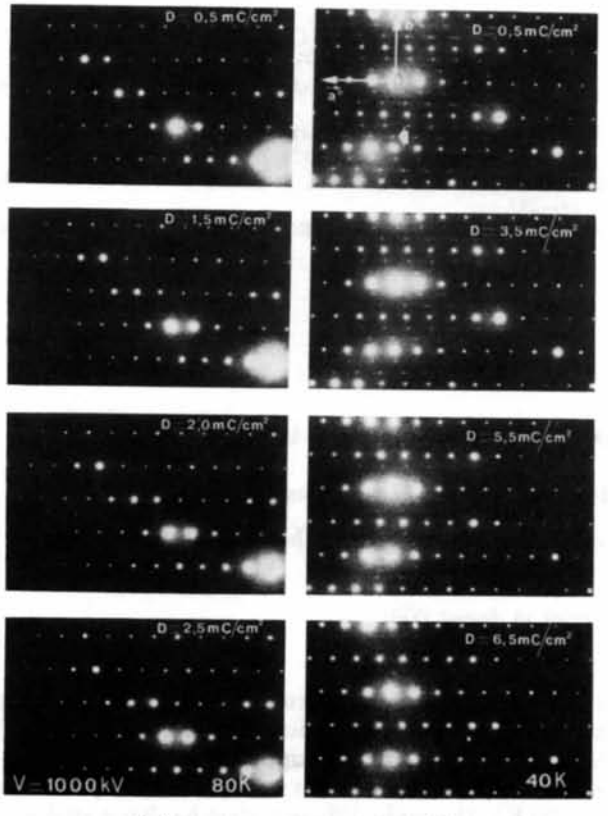

(*a*) (*b*)

Fig. 12. Electron-diffraction pattern at 1000 kV of plane a^*b^*. Changes in intensity of the superstructure spots as a function of the quantity of electrons received by the object. The diffuse streaks are weak and are clear only on the original photographs. (*a*) $T \sim 80$ K. (*b*) $T \sim 40$ K.

Table 5. *Maximum electron doses* (D) (*in* mC cm^{-2}) *for avoidance of loss of coherence between the charge density waves, as a function of the acceleration voltage*

	80 K	40 K
1000 kV	2·0	5·5
2000 kV	3·5	8·5

received by the sample. The satellites (arrows) evolve into weak diffuse streaks (1D order) perpendicular to the **b*** direction, as the irradiation dose increases. This diffusion indicates a loss of the long-range order between charge-density waves carried by the TCNQ organic chain following the formation of defects (Zuppiroli & Bouffard, 1980). An electron dose above 5·5 mC cm^{-2} (or 3·6 e Å^{-2}) destroys all transverse local coherence and only the main reflections can still be observed. At higher temperature, $T = 80$ K (Fig. 12*a*), the three-dimensional order is destroyed by an irradiation dose two and a half times less.

Table 5 indicates – for the working voltages 1000 and 2000 kV used – the critical dose values in mC cm^{-2} determined for two different temperatures: 40 and 80 K.

Changes in and importance of the degree of iodine order

The conditions of synthesis and of crystal growth of the material have a considerable influence on the degree of order of the iodine lattice. The structural arrangement of the iodines for two types of samples has been described:

– those where the iodine has a quasi 1D order, with a large longitudinal coherence length;

– those where the iodine lattice is triply periodic (3D order) with, however, a slight residual amount of 1D disorder; rigorous 3D order was not observed on any diffraction photographs.

Filhol *et al.* (1979) showed that the diffuse layer lines characteristic of a 1D order of lattice (B) do not change as a function of temperature between 100 and 300 K, and as a result no significant change of degree of order was found in this temperature range. The 3D order of lattice (B) is less stable and may be destroyed when the crystal is subjected to constraints. In fact the 3D order decreases:

– progressively if the crystal is subjected to repeated thermal cycles. A dozen of these are sufficient to establish quasi-1D ordering presenting strong correlations in the **a** direction.

– if the crystal is subjected to electron bombardment at room temperature. A crystal placed in a high electron flux under 100 kV for several seconds acquires a 1D order in which the correlations are nevertheless weaker than in the above case.

As shown by X-ray and electron diffraction experiments, the disordered iodine lattice samples do not exhibit the distortion at T_1 as already mentioned by

some of us (Gallois *et al.*, 1983). This is true whether the disorder is due to the method of preparing the samples or to the application of a constraint. This observation suggests that the condition of the appearance of a distortion in the lattice is the existence of a triperiodic iodine lattice. Nevertheless it has not been possible to establish more precisely the relations between the superstructure and the degree of iodine order.

The authors are very indebted to P. Dupuis (Laboratoire de Chimie Physique Macromoléculaire, Nancy, France) who kindly provided the samples and thank C. Coulon (Centre de Recherche Paul Pascal, Talence, France) for very helpful discussions.

References

ABKOWITZ, M. A., EPSTEIN, A. J., GRIFFITHS, C. H., MILLER, J. S. & SLADE, M. L. (1977). *J. Am. Chem. Soc.* **99**, 5304-5308.
ANDRÉ, A., FOURME, R. & RENAUD, M. (1971). *Acta Cryst.* B**27**, 2371-2380.
BRILL, J. W., EPSTEIN, A. J. & MILLER, J. S. (1979). *Phys. Rev. B*, **20**, 681-685.
COPPENS, P., LEUNG, P., MURPHY, K. E., TILBORG, P. R., EPSTEIN, A. J. & MILLER, J. S. (1980). *Mol. Cryst. Liq. Cryst.* **61**, 1-6.
COUGRAND, A., FLANDROIS, S., DELHAES, P., CHASSEAU, D., GAULTIER, J. & MIANE, J. L. (1976). *Mol. Cryst. Liq. Cryst.* **32**, 165-170.
COULON, C. (1983). Ph.D. Thesis. Univ. of Bordeaux I, France.
COULON, C., FLANDROIS, S., DELHAES, P., HAUW, C. & DUPUIS, P. (1981). *Phys. Rev. B*, **23**, 2850-2859.
DUPOUY, G. (1974). *Proceedings of the 3rd International Conference on High Voltage Electron Microscopy*, edited by P. R. SWANN, C. J. HUMPHREYS & M. J. GORINGE, pp. 441-457. London: Academic Press.
DUPUIS, P., FLANDROIS, S., DELHAES, P. & COULON, C. (1978). *J. Chem. Soc. Chem. Commun.* pp. 337-338.
FILHOL, A., GALLOIS, B., LAUGIER, J., DUPUIS, P. & COULON, C. (1982). *Mol. Cryst. Liq. Cryst.* **84**, 17-29.
FILHOL, A. & GAULTIER, J. (1980). *Acta Cryst.* B**36**, 592-596.
FILHOL, A., ROVIRA, M., HAUW, C., GAULTIER, J., CHASSEAU, D. & DUPUIS, P. (1979). *Acta Cryst.* B**35**, 1652-1660.
FLANDROIS, S., COULON, C., DELHAES, P., CHASSEAU, D., HAUW, C., GAULTIER, J., FABRE, J. M. & GIRAL, L. (1981). *Mol. Cryst. Liq. Cryst.* **14**, 663.
GALLOIS, B., COULON, C., POUGET, J. P., FILHOL, A. & DUPUIS, P. (1984). In preparation.
GALLOIS, B., GAULTIER, J., POUGET, J. P., COULON, C. & FILHOL, A. (1983). *J. Phys. C*, **3**, 1307-1312.
GRANIER, T. (1982). Thesis. Toulouse, France.
GRANIER, T. & AYROLES, R. (1982). *J. Phys. (Paris) Lett.* **43**, L285-L290.
GRANIER, T. & AYROLES, R. (1983). *J. Phys. C*, **3**, 1301-1306.
GUINIER, A. (1964). *Théorie et Techniques de la Radiocristallographie*, p. 523. Paris: Dunod.
IKARI, T., JANDL, S. & AUBIN, M. (1983). *Phys. Rev. B*, **28**, 3859-3863.
KHANNA, S. K., POUGET, J. P., COMÈS, R., GARITO, A. F. & HEEGER, A. J. (1977). *Phys. Rev. B*, **16**, 1468-1479.
MEGTERT, S., POUGET, J. P., COMÈS, R., GARITO, A. F., BECHGAARD, K., FABRE, J. M. & GIRAL, L. (1978). *J. Phys. (Paris) Lett.* **39**, L118-L121.
SALIH, S. M. & COSSLETT, V. E. (1975-1976). *Development in Electron Microscopy and Analysis*, edited by J. A. VENABLES, pp. 311-314. London: Academic Press.
SHCHEGOLEV, I. F. (1972). *Phys. Status Solidi A*, **12**, 9-45.
THOMAS, L. E., HUMPHREYS, C. J., DUFF, W. R. & GRUBB, D. T. (1970). *Radiat. Eff.* **3**, 89-91.
YAMAJI, K., MEGTERT, S. & COMÈS, R. (1981). *J. Phys. (Paris)*, **42**, 1327-1343.
YAMAJI, K., POUGET, J. P., COMÈS, R. & BECHGAARD, K. (1983). *J. Phys. (Paris) Colloq.* C**3**, 1321-1323.
ZUPPIROLI, L. & BOUFFARD, S. (1980). *J. Phys. (Paris)*, **41**, 291-297.
ZUPPIROLI, L., MUTKA, H. & BOUFFARD, S. (1982). *Mol. Cryst. Liq. Cryst.* **85**, 1391-1409.

Acta Cryst. (1985). B**41**, 66-76

Chain Ordering in $E_2PI_{1.6}$ (5,10-Diethylphenazinium Iodide)

BY E. ROSSHIRT, F. FREY, H. BOYSEN AND H. JAGODZINSKI

Institut für Kristallographie und Mineralogie der Universität München, Theresienstrasse 41, *D* 8000 *München* 2, *Federal Republic of Germany*

(*Received* 4 *April* 1984; *accepted* 14 *August* 1984)

Abstract

X-ray diffraction patterns of the title compound reveal long-range, short-range and disorder phenomena due to different interactions between and within two sublattices which are incommensurate with one another. A prominent system of diffuse layer lines is due to chain-like inclusions of polyiodide anions. At room temperature doubled and sixfold superperiods along the chains are superimposed. The organic matrix shows a fourfold superstructure along the stacking direction. Lateral correlations are of both short- and long-range type. The description in a frame of uncorrelated sublattices becomes worse at low temperatures ($\lesssim$190 K). The main diffuse system has been analysed in terms of one-dimensional liquid models. The best quantitative agreement was found for an asymmetric distribution function of next-nearest I_3 units, which is intermediate between the classical Zernike-Prins model and a symmetric Gaussian distribution. The

0108-7681/85/010066-11$01.50